Activation energies for vacancy migration, clustering and annealing in silicon

PG Coleman

Department of Physics, University of Bath, Bath BA2 7AY, UK

E-mail: p.g.coleman@bath.ac.uk

Abstract. A series of measurements have been performed at the University of Bath to study the evolution of vacancy-type structures in silicon. Isothermal annealing performed during positron beam-based Doppler broadening measurements have yielded activation energies for vacancy cluster formation and evaporation in silicon of approximately 2.5 and 3.7 eV, respectively. The clusters, which could predominantly be the stable hexavacancy, appear to form between 400-500ºC, and anneal at ~ 600ºC. A similar technique applied to low-temperature *in situ* measurements have yielded the migration energies for the silicon monovacancy and interstitial (of ~ 0.5 and 0.08 eV, respectively). Interesting observations of positronium formation at the surface of the samples studied during isothermal annealing are presented.

1. Introduction

For many years researchers – including many using positron beam spectroscopy - have studied the thermal evolution of vacancy-type defects in ion-implanted silicon [1-3]. There appears to be a consensus (a) that the defects left in room-temperature silicon are predominantly divacancies (V_2), (b) that at 200-300ºC V_2 become mobile and migrate to sinks or – if their concentration is high enough – agglomerate to form small clusters, (c) that at 400-500ºC even larger clusters are formed, and (d) that at ≥ 600ºC these large clusters are annealed. There have been observed differences between these behaviours in different types of silicon (e.g., float zone (FZ), Czochralski (Cz), highly-doped [4,5]), and some debate concerning the various stages of evolution, especially stage (b) – where positron annihilation spectroscopies (both lifetime and Doppler broadening) have in some studies implied that the V_2-like response has survived to temperatures well above that accepted for V_2 migration, while other techniques applied in parallel have indicated their disappearance [6].

There is also the question of possible differences between the evolution of V_2 in the bulk and near the surface of silicon, and the dependence on V_2 concentration. Although lifetime spectroscopy is held to yield greater insights into the sizes and relative concentrations of open-volume point defects in silicon, we shall consider in this paper the application of single-detector Doppler broadening spectroscopy (formally called variable-energy positron annihilation spectroscopy, VEPAS, and sometimes variable-energy Doppler broadening of annihilation radiation, VEDBAR) to identify various small vacancy clusters and, as it continues to provide the fastest method for following *changes* in defect structure during, for example, annealing, to deduce activation energies for various processes involved in vacancy evolution.

2. Experimental details

All the measurements described here were performed on the magnetic-transport positron beam at the University of Bath, full details of which can be found elsewhere [7]. Positrons from a ^{22}Na source are moderated by annealed tungsten meshes and transported magnetically to the sample, mounted on 0.1 mm-diameter tungsten wires, via an ***E×B*** velocity filter through which unmoderated positrons are not transmitted and an accelerator section which determines the final incident positron energy. Because the electrostatic accelerating field (potential difference V) and guiding magnetic field are not perfectly aligned the positron beam moves laterally as V is changed; the beam is brought back to the same position at the sample target by two orthogonal trim coils. The beam is positioned using a small washer-shaped dummy sample and observing the image created by those positrons which pass by the target and proceed along a beam dump line to a dual electron multiplier array mounted in front of a phosphor screen. The energy spectra of annihilation gamma photons from the sample are measured by a Ge detector, and the Doppler-broadened linewidth parameters S and W [8] are measured for each incident positron energy. Any positron which misses the sample – for example, if the sample is slightly smaller than the 8mm-diameter beam - decay on at the end of the beam dump, out of sight of the gamma detector. The probability of detection of annihilation photons from backscattered positrons is minimized by the use of a large sample chamber. Beam energy and position, together with all aspects of data collection, are computer-controlled. Individual run times are chosen so that ~ 10^6 events are recorded in each annihilation line, and are ~10^3 s.

All Si samples (except those discussed in section 4.2) were ion-implanted at room temperature at the Surrey Ion Beam Centre (Nodus Laboratory, under the direction of Professor Russell Gwilliam). Typical sample sizes were ~ 10x10mm, although sizes ranging from 5x5 to 20x20mm have been used.

3. Isochronal annealing studies

Almost all previous work using positrons has been in this category. With the exception of He-implanted Si, where the ramp annealing rate is important in void growth mechanisms [9], samples are usually held at the chosen temperature for a set time and the ramp rate is not considered important. In the first example we consider FZ Si samples implanted with 50 keV Si^+ ions at a dose of 5x10^{13} cm^{-2} and annealed for 30s at temperatures between 250 and 850ºC. The raw data (S parameter vs incident positron energy E) are shown in Fig. 1 [10], normalised to the value for bulk Si. The peak in $S(E)$ represents the non-saturated VEPAS response to divacancies (which have a characteristic S value of ~1.04). The data show that there is no measurable change in VEPAS response for samples annealed to 450ºC, with a rapid change at 550ºC and essentially complete annealing at 650ºC and above. This result was confirmed by in-situ annealing experiments by measuring the fraction of implanted positrons able to diffuse to the surface as the temperature was raised (via measurement of the amount of positronium formed at the surface). The result is surprising at first sight because V_2 should be

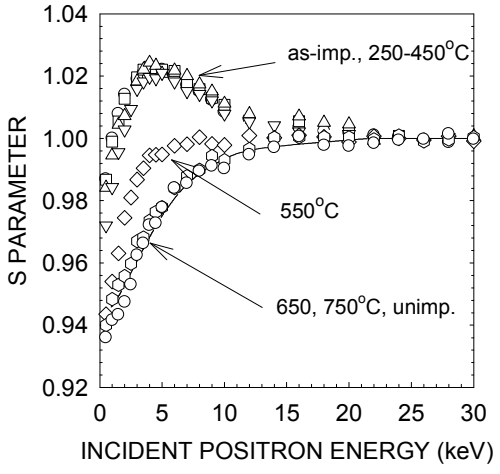

Figure 1. $S(E)$ for FZ Si implanted with 50 keV Si^+ ions at 5x$10^{13}$$cm^{-2}$ and annealed at temperatures from 250 to 750ºC [10].

mobile at ~ 300ºC and annealing should therefore progress at this temperature. As for clustering (agglomeration), one might still expect to see a change in $S(E)$ as this progresses, for the following reasons.

The conventional model describing VEPAS response to clustering states that (a) the S value characteristic of V_n (a cluster of n vacancies) increases with n, and the specific positron trapping rate ν_n for V_n is ~ $n\nu_1$, where $\nu_1 \approx 3.4 \times 10^{14}$ s^{-1}. Let us consider here the dependence of S on n for Si. Here we attempt to apply the dependence on n of the positron lifetime results of Staab *et al* [11], assuming an asymptotic value of 499 ps (the spin-averaged lifetime of positronium) with the calculations of S by Hakala *et al* [12] convoluted with our experimental detector resolution. This is reasonably straightforward for low n, but extrapolation to large clusters is difficult and the fit in figure 2 should be taken with caution. The asymptotic value of S at large n here is suggested to be 1.13, close to the largest values measured directly (see, for example, ref [8]); however, a value somewhat higher than this may be possible.

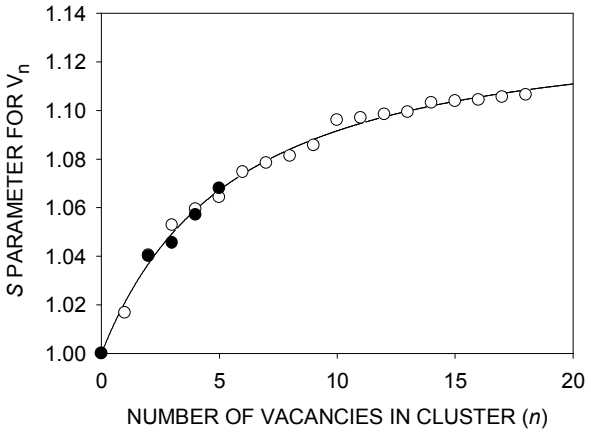

Figure 2. S parameter characteristic of vacancy clusters V_n vs n. Black circles: convoluted calculations of Hakala *et al* [12]. Open circles: normalised positron lifetime results of Staab *et al* [11]. Asymptotic S value (large n) = 1.13.

The total positron trapping rate is νC, where C is the defect concentration per atom. Therefore, if *all* the V_2 agglomerate into clusters V_n, the trapping rate is $\nu_n C_n = (n/2)\nu_2\ (2/n)C_2 = \nu_2 C_2$ – i.e., it remains unchanged; however, S_n is larger than S_2 and so the measured S value should increase. This is the case even if the simple proportionality between ν_n and n is too crude an approximation.

Let us consider four possible models which might explain why this is not the case. (a) Only a fraction of the V_2 cluster and the rest diffuse to sinks (particularly the surface). For the measured S value to remain unchanged then the increase in S_n resulting from clustering would have to be balanced exactly by the decrease in C. This is possible but an exact balance is nevertheless unlikely. (b) The V_2 are pinned by impurities and become mobile at higher temperatures than the 300ºC expected. This model is also not very convincing because we are using FZ Si and the impurity concentrations are expected to be too low to pin all the V_2. (c) The V_2 do cluster, say to V_4, but the S value does not change measurably; this is the scenario invoke by Poirier et al. [6] to explain a similar observation after measuring no significant change in positron lifetime on annealing. This is contrary to the $S(n)$ dependence suggested by figure 2; if it were to be the case then the clusters would have to have a structure different from that assumed in the calculations shown in the figure – as suggested by Poirier et al. - for example, a linear structure whose S value was similar to that for V_2. Another possibility, earlier proposed by Poirier *et al* [13] is that V_2 for 'virtual' clusters – i.e., they form loose connections without close bonding, so that they become less mobile but positrons are still trapped in a defect of the size of V_2 and thus the annihilation parameters remain unchanged. (d) The initial defects are not V_2 but are already an array of small clusters which are not mobile below 500ºC. While possible, this is

unlikely as there have been a large number of positron measurements indicating that the defects remaining in ion-implanted Si at room temperature are overwhelmingly V_2.

In order to remove the possible complications associated with the close proximity of the surface, measurements on 4MeV Si-implanted FZ Si have been performed [14]. Here the peak of the damage created by the ion implantation is close to 2.5 μm below the surface. Figures 3 and 4 show $S(E)$ for implant doses between 10^{12} and 10^{14} cm^{-2} before an after 30 mins one-shot annealing to 600ºC, respectively. Comparison of the two figures leads to the conclusion that the V_2 formed at depths from the surface to ~2 μm are annealed below 600ºC, but that between 2-3 μm a layer of small clusters is formed which survives to higher temperatures. By fitting the data shown in figure 3, and those obtained by employing an etch-and-measure technique to bring the damaged layer progressively towards the surface, with the standard code VEPFIT [15], the average size of the defects in this buried layer is suggested to be 3.5 – i.e., most likely dominated by tetravacancies. It was also found that progressive annealing up to 600ºC removed all VEPAS response to vacancy-type damage, confirming that cluster formation is critically dependent upon annealing history.

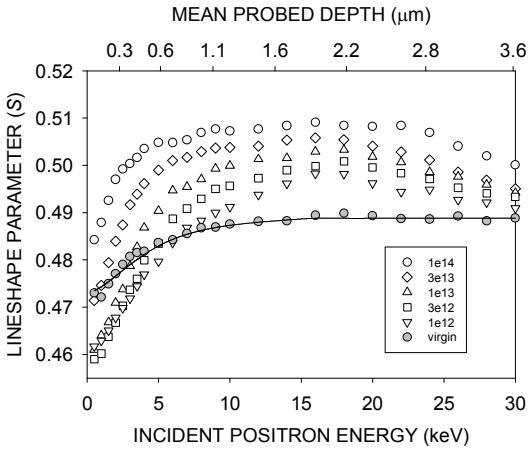

Figure 3. $S(E)$ for 4MeV Si ions in Si at doses from 10^{12}-10^{14} cm^{-2} (1e12-1e14) [14].

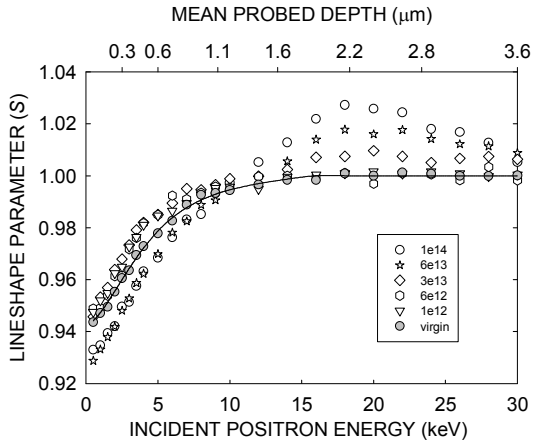

Figure 4. As figure 3, after one-shot annealing for 30 mins at 600ºC [14].

The explanation for the formation of small clusters in the 2-3 μm region is most likely linked to the initial distribution of vacancies following implantation. A simulation for 4MeV Si^+ in Si using the code SRIM [16] is shown in figure 5. The concentration of vacancies in the 2-3 μm region is almost an order of magnitude higher than in the tail stretching to the surface; it is therefore considerably more likely that V_2 in the former region find each other on migrating at high temperatures than in the latter –

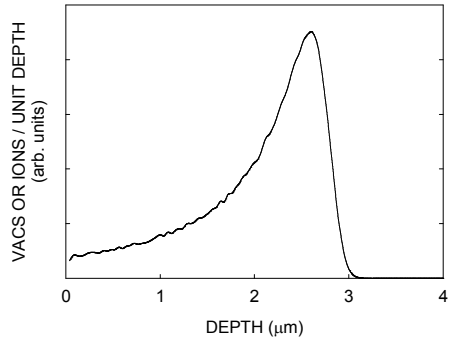

Figure 5. SRIM simulation of vacancy damage in Si implanted with 4MeV Si^+ ions.

which, additionally, is closer to the surface sink. On extracting a defect concentration in the buried layer from data fitting, one obtains a super-linear dependence on ion dose which is consistent with the probability of agglomeration depending on the relative magnitudes of the mean divacancy separation and the diffusion length of the migrating V_2.

4. Isothermal annealing studies

4.1. Divacancy evolution

The first isothermal annealing studies in the author's laboratory aimed at extracting more information on the thermal evolution of vacancy defects in Si were performed on 2MeV Si-implanted Cz Si [17]. A high dose of 10^{15} cm^{-2} ensured that the V_2 concentration was high enough to lead to agglomeration, and the 2 MeV ion energy meant that the damage extended to depths where positron (and V_2) diffusion

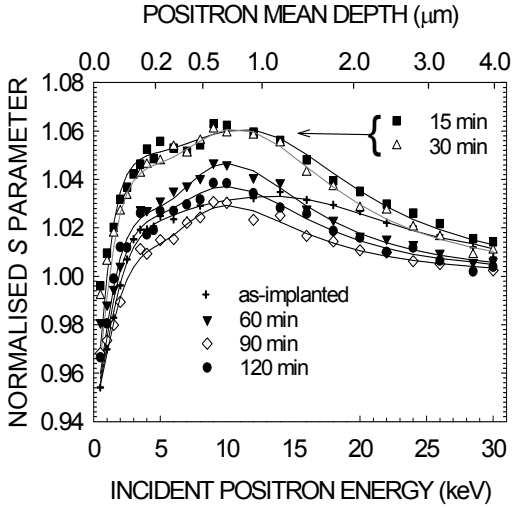

Figure 6. Normalized $S(E)$energy for Cz Si implanted with 2 MeV, 10^{15} $Si^{+}cm^{-2}$ after annealing at 600°C for different time intervals. The solid lines are fits using VEPFIT. Adapted from [17].

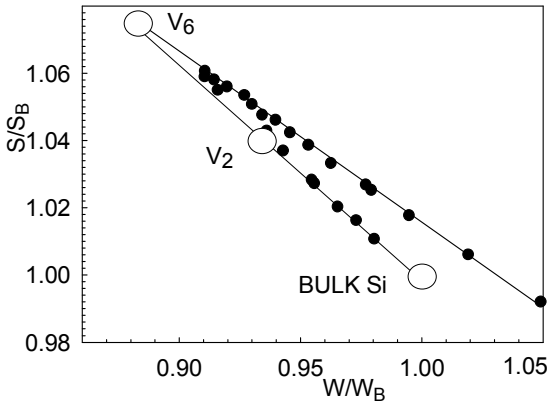

Figure 7. *S-W* plots for samples implanted with 2 MeV Si ions at 10^{15} cm^{-2} dose after annealing at 600°C for 30 min. The circles are the dominant annihilation sites for positrons. Adapted from ref [17].

to the surface might not present significant interpretational problems when analyzing the data.

Examples of the data taken are shown in figure 6. $S(E)$ for the as-implanted sample (crosses in figure 6) show a broad peak with a maximum response of ~ 1.03 at E ~ 15 keV (equivalent to a mean positron implantation depth of ~ 1.3 μm). On annealing at 600ºC for times up to 30 mins S increases remarkably at all E, pointing to the formation of clusters, particularly at depths ~ 750 nm, where there is a broad peak in the response. On annealing for longer times the response decreases and the shape of $S(E)$ becomes progressively more peaked at ~ 10 keV (~ 750nm), a response which survives annealing for 2h.

Data such as those in figure 6 are routinely fitted with the code VEPFIT, which gives values for S and for the positron diffusion length (L) in each layer (the S value would only be measured if at some energy E all the positrons were annihilated in the layer; this is not generally the case). A graphical equivalent of VEPFIT is the parameter-parameter map – illustrated by the *S-W* plot in figure 7. Here the parameters S and W for every value of E are plotted against each other. On such a graph can be plotted points which are characteristic of each layer – and additionally of each 'pure' annihilation state (sample surface, bulk Si, V_2, etc). In figure 7 the surface state is in the bottom right-hand corner of the

graph, and the *S*,*W* points for bulk Si and annihilations in V_2 are represented by circles. If the linear trends suggested by the data points are extrapolated as shown in figure 7, then they meet at the *S*,*W* point characteristic of a defected layer, even if experimentally positrons do not all suffer annihilation in the layer. In this case the straight lines meet at $S \sim 1.075$, which is the value predicted in figure 2 for the hexavacancy V_6. The data are thus consistent with saturation trapping of those positrons which are annihilated in the layer centred at ~ 750 nm in defects of the size of V_6.

Let us now turn to the time dependence of the evolution seen in figure 6. In these experiments the concentration of defects (C_D) was first deduced by remembering that the *S* value for a layer in which defect trapping sites exist with a characteristic $S = S_D$ is a linear combination of S_D and S_B, where S_B is the *S* value for bulk Si, which is normalised to unity here: $S = fS_D + (1-f)$. *f*, the fraction of positrons annihilated in the layer from the trapped state, is linked to C_D via $f = \nu C_D/(\lambda+\nu C_D)$, where ν is the specific trapping rate for the defects in question and λ is the positron annihilation rate in bulk defect-free Si. By inserting this expression for *f* into that for *S* one arrives at

$$C_D = \lambda(S - 1)/[\nu(S_D - S)] \quad . \tag{1}$$

At a given temperature T one can now measure the time $t_{1/2}$ taken for C_D to decrease to 50% of its room-temperature value. If we assume that at a temperature *T* C_D decreases as

$$C_D = C_0 \exp(-E_A/k_B T) \quad , \tag{2}$$

where C_0 is the defect concentration at time zero and E_A is the activation energy for the annealing process, then the slope of an Arrhenius plot of $\ln(t_{1/2})$ vs $(1/T)$ should yield E_A. In the case of the data shown in figure 6 ($T = 873$K), $t_{1/2} \approx 39$ min (see figure 8).

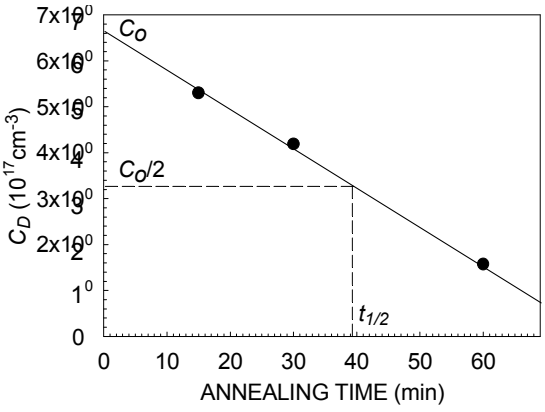

Figure 8. Defect concentration C_D (cm^{-3}) deduced from the data in figure 6 vs annealing time at 600ºC. The vacancies are assumed to be all V_6 [17].

Unfortunately, there were not enough data points to enable the unambiguous extraction of E_A for the annealing of the vacancy clusters (assumed to be V_6) formed in this experiment. An upper limit of 7.5 min could be assigned to annealing at 700ºC, and the annealing at 650ºC was complicated by the possible presence of a mixture of V_6 and smaller clusters, so that the analysis could only suggest a minimum value for E_A of 1.2 eV. This is considerable lower than the figure of ~ 3.5 eV postulated for the binding of V to V_6 [11,18-20] and of the same order as E_A for V_2 migration [21]. A further series of experiments was therefore performed to endeavour to resolve these problems.

A set of samples of Cz and epitaxially-grown Si were implanted with 50keV Si^+ ions at a dose of 5 x 10^{13} cm^{-2}. The samples were then isothermally annealed *in situ* (i.e., on the sample holder at the target position in the positron beam system) at temperatures between 300 and 640ºC for times of up to ~ 100 h, and the value of *S* at a positron energy equivalent to a probed depth similar to that predicted by SRIM to be the depth at which the vacancy-type damage was a maximum (i.e. 3.5 keV, equivalent

to 120nm) recorded every 600s (reduced to 300s at the highest temperatures) [22]. The $S(E)$ plots shown in figure 9 were taken after S(3.5 keV) had stopped changing in the epi-Si samples held at 470 and 580ºC; the samples were cooled to room temperature before the data were recorded. Note that the samples were in this case not HF-etched to remove surface oxide, to increase the absolute size of the change in S; as a test, other measurements were taken after etching and no effect on the final results was noted.

Examples of S(3.5 keV) vs time plots are shown in figure 10. Data were also taken at E = 1 and 24

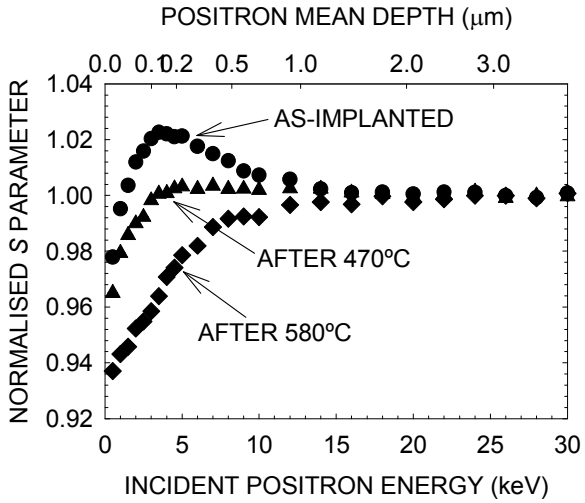

Figure 9. $S(E)$ for epi-Si implanted with 50keV Si^+ ions at a dose of $5x10^{13}cm^{-2}$, as-implanted and after annealing at 470 and 580ºC. Adapted from [23].

keV to check for physical changes near the surface and systematic changes (e.g. in the detector/amplifier performance). The three plots in figure 10 illustrate the three temperature regions of interest. At temperatures below ~ 400ºC essentially no change is seen in the value of S, in line with earlier observations. Between ~ 400 and 500 ºC S falls to an intermediate level (here coincidentally ~1 – see figure 9). Between ~ 500-600 ºC the defects are annealed away and the positron response falls to that for unimplanted Si (at 3.5 keV this is ~ 0.97 here).

The fall in S at higher temperatures reflects the change in the defect structure; at 470ºC in

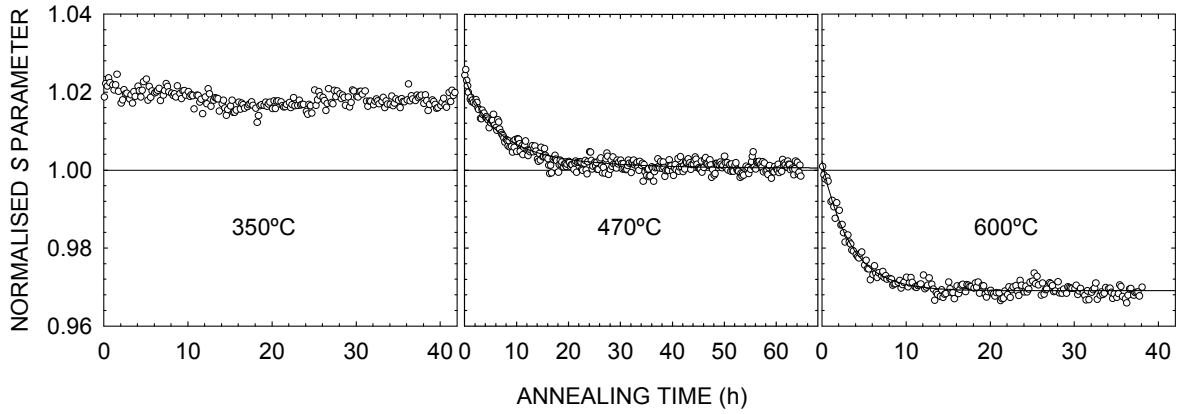

Figure 10. S(3.5 keV) vs annealing time for implanted epi Si at 350, 470 and 600ºC. The solid lines through the points in are exponential fits. S values are normalised to that for bulk Si (i.e., unity – as shown in the graphs). Adapted from [23].

figure 10, for example, the peak S falls to an equilibrium value characteristic of an intermediate state. The fact that S falls (i.e., as opposed to rises) indicates that any changes have involved a decrease in the trapping rate, or a sublinear increase in defect S value with defect size, or the migration of some V_n to sinks, or a combination of these processes. In principle it does not matter whether S increases or decreases; it is the ability to extract a time rate of change of S which is important here. Thus, if plots of $S(t)$ such as those shown in figure 10 are fitted to an exponential $S_0\exp(-\lambda t)$, the decay constant λ represents the change which is occurring, and can be used in Arrhenius plots to evaluate the activation energy for the process. Figure 11 shows such plots for the low and high temperature regions (400-500ºC and 560-640ºC) for both Cz Si and epi-Si.

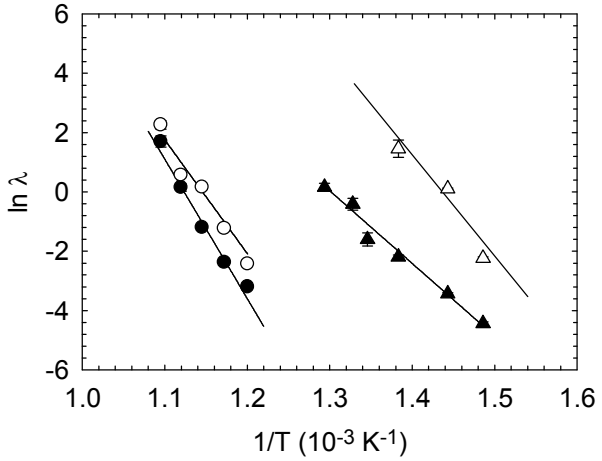

Figure 11. Arrhenius plots for epi and Cz-Si samples. The slopes of the fitted lines give activation energies for two vacancy evolution processes (lower temperatures, triangles and higher temperatures, circles). Solid symbols – epi-Si: open symbols – Cz Si. From [23].

The activation energies E_A obtained the gradients of the lines fitted to the data in figure 11 are 2.1 (2) and 2.7 (7) eV for the low-temperature process, and 3.9 (3) and 3.6 (3) eV for the high-temperature process, the first values being for epi-Si and the second for Cz Si.

4.2. Monovacancy evolution

Studying monovacancies (V_1) in Si with VEPAS presents the practical problem that V_1 are mobile below room temperature, which is the reason why room-temperature samples contain predominantly V_2 (with the possibility of small clusters for samples implanted with ions at high doses). In order to observe the formation and annealing of V_1 the Si sample was mounted in the Bath positron beam on a copper cold finger attached to the head of a closed-cycle helium cryostat [23]. The 25mm-diameter copper rod was broken by a 0.3mm-thick sapphire disk, affording good thermal and poor electrical conductivity. The Si sample was cooled to below 20K and was held at -20kV while low-density He gas was admitted to the sample chamber; He ions were accelerated into the sample from the ensuing discharge. A measure of $S(E)$ after implantation showed a peak between 2 and 4 keV (mean depth ~ 130nm, consistent with 20keV He implantation), close to the saturation value of 1.027 (assigned to V_1).

Two types of Si – low-impurity FZ Si and highly As-doped (n^+) Si – were studied in these experiments [24]. S(3.5 keV) was, as in the V_2 experiments in subsection 4.1, monitored as a function of time for periods of up to 6 days at a range of constant temperatures from 200K to over 300K. Figure 12 shows examples of raw data for FZ and n^+ Si. In n^+ Si two processes in different temperature ranges were observed directly, whereas in FZ Si both processes could proceed at the same temperature.

The Arrhenius plots obtained by plotted the natural logarithm of the decay constant representing the time rate of change in S (shown to be proportional to that for the change in defect concentration) are shown in figure 13, therefore consist of two straight lines for n^+ Si and a nonlinear plot for FZ

which tends to one slope at low temperatures and a higher slope at higher temperatures, as the relative probability of the two processes changes. Note that the uncertainties attached to the measurements of the first stage of annealing of defects in n^+ Si were too high for data to be included in figure 13. The

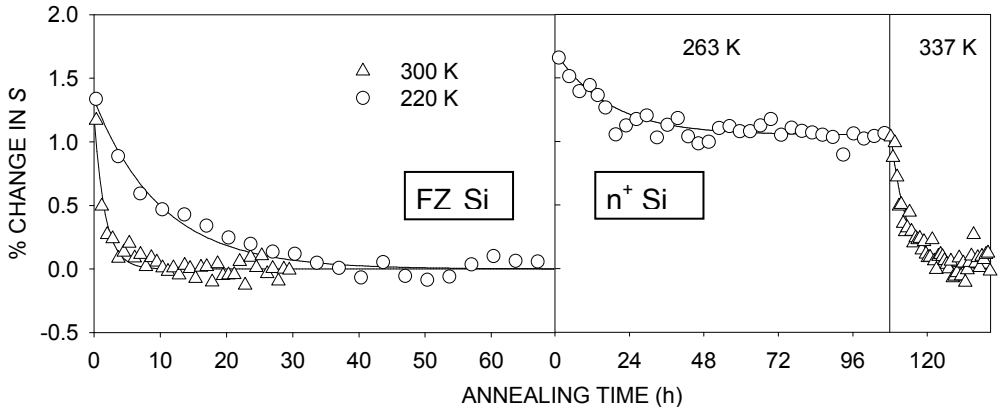

Figure 12. Percentage difference between S parameter at E = 3.5 keV for low-temperature He-implanted FZ and n^+ Si and its asymptotic value as a function of time at four temperatures. Adapted from [24].

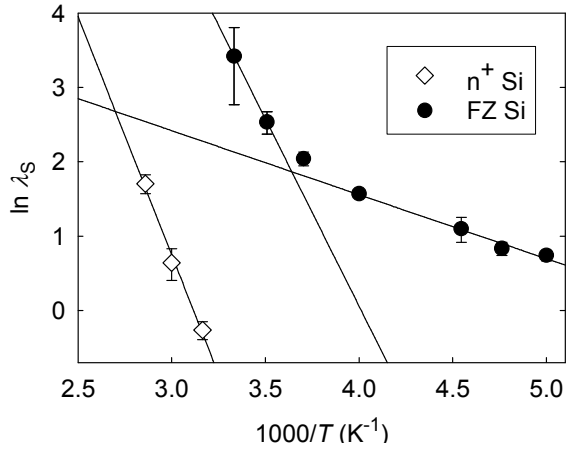

Figure 13. Arrhenius plots of $\ln\lambda_S$ vs $1000/T$ for low-temperature He-implanted FZ and n^+ Si, where λ_S is the decay constant from exponential fits of data such as those in figure 12, and T is the absolute temperature in K [24].

activation energies derived from the slopes of the fit lines in figure 13 were 0.078(7) and 0.46 (28) eV for FZ Si, and 0.59 (6) eV for n^+ Si. Let us now proceed to discuss the activation energy results in the following section.

5. Activation energies

The Arrhenius plots in figures 11 and 13 yield activation energies for processes involving the evolution of vacancy-type defect structures in different types of silicon and over different temperature ranges. The challenge of identifying the most likely candidates for these processes is not simple, and we can only at this stage offer what appears to be the most likely. The most straightforward interpretation is that for the high-temperature process in figure 11. The measured activation energy of about 3.75 eV for both epi and Cz Si describes the disappearance of the VEPAS response to defects in the samples, and lies in the range of published values for the binding energy of vacancies to small clusters [11,18-20], particularly the 3.76 eV calculated by Hastings et al for the hexavacancy. This

high-temperature process is therefore likely to be the evaporation of clusters – the hexavacancy is the most probably candidate here – via the removal of successive vacancies which are then able readily to migrate to sinks.

The lower-temperature process seen in both Cz and epi-Si, with activation energies of ~ 2.5 eV, is more difficult to interpret. The transition from V_2 to the clusters which evaporate at higher temperatures is the most likely explanation, but this does not easily sit with the accepted knowledge that V_2 migrate at or below 300ºC, or that the migration energy for V_2 is 1.3 eV [21]. One therefore has to introduce the possibility that V_2 may first undergo some kind of transition into small clusters - say V_4 – which may exists in an unstable chain-like form as proposed by Poirier et al. [6], with a negligible change in the VEPAS response. At the temperatures studied this agglomeration may happen very rapidly. 2.5 eV may then be a measure of the migration energy of V_4. The agglomeration occurring between 400-500ºC proceeds measurably more quickly in Cz Si than in epi-Si at the same temperatures; this could be due to the action of impurities as seeds for cluster formation.

The plots in figure 13 also suggest the existence of two steps in the annealing process for (neutral) V_1 in Si, with activation energies of about 0.08 and 0.5 eV. The fact that the two processes appear to dominate in different temperature ranges suggests that the former involves a higher number of steps than the second. Comparison with well-accepted values [25] suggests that the high-temperature process is associated with neutral V_1 migration. This energy has been measured previously by EPR and other spectroscopies. However, more importantly, the other process (with the 0.08 eV activation energy) is attributed to the migration of Si interstitials. This energy is very difficult to measure and has been the subject of much debate over recent decades; the VEPAS value agrees within uncertainties with that measured by Hallén et al. [26] and may go some way towards ending the debate in this area.

The survival of a fraction of vacancies formed in highly As-doped n^+ Si (figure 12) is consistent with the scenario in which a significant fraction of the V_1 form complexes with the dopant impurities [4] and thus consequently become considerably less mobile.

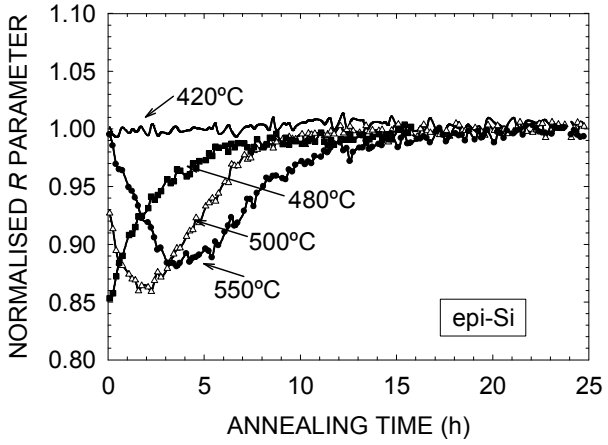

Figure 14. Normalised *R* parameter as a function of annealing time for epi-Si samples at four temperatures. The sample at 420ºC was unetched prior to the measurements.

6. Loose ends

A number of unexpected and interesting observations were made during the isothermal annealing studies described in section 4. Perhaps the most intriguing was the behaviour of the peak-to-valley ratio, defined as the ratio of the total counts in the annihilation line (Ge detector photopeak centred at 511 keV) divided by those in the ('valley') region immediately to the left of the photopeak. This ratio has long been used as a measure of the amount of positronium (Ps) formation at the surface of a metal or semiconductor sample, enhanced at elevated temperatures by the desorption of positrons trapped in the surface as thermal Ps [27]. The peak-to-valley ratio, which we shall here call *R*, was measured

automatically along with the *S* and *W* lineshape parameters; as the system was set up for measurement of these parameters the extent of the valley region was smaller than would normally be used – however, *R* could be measured with relatively high precision as a function of time at each temperature.

Figure 14 shows an example of the behaviour of *R* in four samples of implanted Si during isothermal annealing. The values are normalised to that for bulk Si (measured directly by implanting room-temperature samples with 25 keV positrons, so that a negligible fraction of the implanted positrons are able to diffuse back to the surface to form Ps). The fraction of positrons forming Ps at the surface of the samples is clearly varying significantly with time, increasing as *R* decreases and tending to zero for each sample at long times.; the exception is the sample annealed at 420ºC, which had not been etched using HF prior to the measurements. It is not unexpected that the Ps fraction greatly depends on the presence or otherwise of native oxide on the surface of the Si; what is not currently understood by the author is the cause of the variation of Ps formation with time at the various temperatures. One notes that the variation does not show a clear trend with annealing temperature, and so must critically depend on the nature of the individual surfaces of each sample. The presence of native oxide seems to prevent, or at least greatly reduce, the variation seen. Oxidation may hold the key, but it is yet to be confirmed that oxide growth, or the state of the oxide-Si interface, may vary in such a way to explain the observed data. It is also possible that heating is creating changes in formation potential for Ps at the surface. These observations may have a prosaic or an exotic explanation; in either case they warrant further investigation.

7. Conclusions

This paper has tried to summarise the current situation with regard to the study of vacancy-type defect evolution at the University of Bath. There are many pitfalls and potential problems with making measurements at high temperatures, both practical and interpretational, and the conclusions summarised above must be taken in the spirit of work in progress. However, the extraction of activation energies has not been widely performed with beam-based positron spectroscopies and it is to be hoped that this work will encourage more researchers to consider applying this method to gain information on defect evolution not only in semiconductors but also in metals, alloys and other solid materials. Caution must always be invoked in these studies; for example, positron detrapping from defects could affect the results (in a recent paper Makkonen and Puska [28] predict an extremely small binding energy – perhaps a few tens of meV - for positrons in neutral Si monovacancies). There may be much more scope for working at low temperatures, perhaps by incorporating a positron beam into an ion implanter and performing measurements with the samples in situ; and the unambiguous identification of vacancy cluster size may require the application of beam-based positron lifetime spectroscopy (VEPALS). It is clear that there is still much interesting work to be done in this area.

Acknowledgements

The author is grateful to the many people who have contributed in various important ways to the research reported in this paper. Drs Dana Abdulmalik, Paul Burrows, Ruth Mason, Ruth Harding and Ilham Al-Qaradawi, and Prof. Gordon Davies, were directly involved in taking and analysing data and in the many discussions which followed, and Nathan Potter worked on void formation in He-implanted Si. I am especially grateful to Dr Andy Knights for many stimulating discussions and ideas. Most of the ion implantion of samples was performed at the Surrey Ion Beam Centre. Work at the positron laboratory of the University of Bath was supported financially by EPSRC, UK throughout the time of the work reported herein, for which the author is grateful.

References

[1] Simpson P J, Vos M, Mitchell I V, Wu C and Schultz P J 1991 *Phys. Rev.* B **44** 12180
[2] Fujinami M, Tsuge A and Tanake K 1996 *J. Appl. Phys.* **79** 9017
[3] Nielsen B, Holland O W, Leung T C and Lynn K G 1993 *J. Appl. Phys.* **74** 1636

[4] Ranki V, Nissilä J and Saarinen K 2002 *Phys. Rev. Lett.* **88** 105506
[5] Dannefaer S, Avalos V, Kerr D, Poirier R, Shmarovoz V and Zhang S H 2006 *Phys. Rev.* B **73** 115202
[6] Poirier R, Avalos V, Dannefaer S, Schiettekatte F and Roorda S 2003 *Physica* B **340-2** 609
[7] Chilton N B and Coleman P G 1995 *Meas. Sci. Technol.* **6** 53
[8] van Veen A, Schut H and Mijnarends P E 2000 *Positron Beams and their Applications* ed P G Coleman (World Scientific: Singapore) p 191
[9] Ruffell S, Simpson P J, Knights A P 2007 *J.Phys.: Condens. Matter* **19** 466202
[10] Coleman P G, Malik F and Knights A P 2002 *J.Phys.: Condens. Matter* **14** 681
[11] Staab T E M, Sieck A, Haugk M, Puska M J, Frauenheim Th and Leipner H S 2002 *Phys. Rev.* B **65** 115210
[12] Hakala M, Puska M J and Nieminen R M 1998 *Phys. Rev.* B **57** 7621
[13] Poirier R, Avalos V, Dannefaer S, Schiettekatte F and Roorda S 2003 *Nucl. Instrum. Methods* B **206** 85
[14] Coleman PG, Harding R E, Davies G, Tan J and Wong-Leung J 2007 *J. Mater. Sci. Electron.* **18** 695
[15] van Veen A, Schut H, De Vris J, Hakvoort R A and Ijpma M R 1990 *AIP Conf. Series* **218** 171
[16] Ziegler J 2005 www.srim.org
[17] Abdulmalik D A, Coleman P G and Al-Qaradawi I Y 2006 *Appl. Surf. Sci.* **252** 3209
[18] Hastings J L, Estreicher S K and Pedders P A 197 *Phys. Rev.* B **56** 10215
[19] Makhov D V and Lewis L J 2004 *Phys. Rev. Lett.* **92** 255504
[20] Kalyanaraman R, Haynes T E, Holland O W, Gossman H-J L and afferty C S 2001 *Nucl. Instrum. Methods* B **175-7** 182
[21] Watkins G D and Corbett J W 1965 *Phys. Rev.* **138** A543
[22] Abdulmalik D A and Coleman P G 2008 *Phys. Rev. Lett.* **100** 095503
[23] Mason R E and Coleman P G 2006 *Appl. Surf. Sci.* **252** 3228
[24] Coleman P G and Burrows C P 2007 *Phys. Rev. Lett.* **98** 265502
[25] Watkins G D 2000 *Mater. Sci. Semicond. Process.* **3** 227
[26] Hallén A, Keskilato N, Josyula L and Svensson BG 1999 *J. Appl. Phys.* **86** 214
[27] Mills A P Jr 1995 *Positron Spectroscopy of Solids* ed A Dupasquier and A P Mills Jr (IOS: Amsterdam) p 209
[28] Makkonen I and Puska MJ 2007 *Phys. Rev.* B **76** 054119